Supplementary Information (SI) for ChemComm.
This journal is © The Royal Society of Chemistry 2026

Supplementary Information

Tuning Photocatalytic CO_2 Reduction Reaction Performance via Nodes and Dimensionality in Metal-Organic Frameworks

Xin Lu[#], ChenLi Wang[#], Xinyi Wu, Wenjing Liu and Chuan-Lei Zhang*

Anhui Provincial Key Laboratory of Advanced Catalysis and Energy Materials, Anhui Ultra High Molecular Weight Polyethylene Fiber Engineering Research Center, School of Chemistry and Chemical Engineering, Anqing Normal University, Anqing 261433, P. R. China. E-mail: clzhang@nju.edu.cn.

1. Materials and methods.

Materials and equipment. All chemicals were obtained from commercial sources and used without further purification. XRD was performed using a Bruker D8 Advance X-ray diffractometer equipped with a Cu target from SHIMADZU, Japan, with Mo-Kα (λ = 0.71073 Å) radiation and an X-ray tube operating at 40 mA / 40 kV. Using 5 mg of sample mixed with 500 mg of KBr microspheres, a Nicolet (AVATAR 360) type spectrometer was used to record infrared absorption spectra in the wave number range 400 ~ 4000 cm^{-1}. The synthesised materials were analysed for C, H and N using a Perkin Elmer 240C elemental analyser. Thermogravimetric analysis (TGA) was carried out using a simultaneous thermal analyser in STA409PC with an adjustable temperature range up to 973 K and a heating rate of 10 K min^{-1} under N_2 atmosphere. Fluorescence spectra and ion detection were performed on a fluorescence spectrophotometer (model LS 55, Perkin-Elmer). Determination of solid-state fluorescence decay lifetimes of samples using the FLS920P fluorescence spectrometer supplied by Edinburgh Instruments. Liquid phase UV-visible absorption spectra were recorded with a Shimadzu UV-2700 spectrophotometer. Solid phase UV-visible absorption spectra were recorded with a Shimadzu UV-3600 spectrophotometer. Solid phase UV-visible absorption spectra were recorded with a Shimadzu UV-3600 spectrophotometer using $BaSO_4$ as a reference. Gas chromatography (GC) was characterised by a GC-7860 Plus instrument.

Synthesis of TTZ. Using an electronic balance, 9.64 g of tris(4-bromophenyl)amine (20.0 mmol), 13.80 g of 1,2,4-triazole (200.0 mmol), 0.19 g of CuI (1.0 mmol), 0.53 g of 18-crown ether-6 (2.0 mmol), and 27.6 g of K_2CO_3 (200.0 mmol) were weighed and all the samples were suspended in 100 mL of DMF solution. The mixture was placed in a 250 mL two-necked round-bottomed flask, evacuated and passed through N_2 to ensure oxygen-free conditions, and heated to 160 °C under N_2 protection with condensation and reflux for 3 days, and then cooled to room temperature at the end of the reaction. The solvent was removed by spin distillation and the reaction mixture was added to 200 mL of H_2O, washed with water and filtered and dried in vacuum to obtain a light blue powder. The crude product was separated by column chromatography (ethyl acetate/methanol = 5:1) to give a light pink crystalline powder 6.96 g (about 78% yield based on tris(4-bromophenyl)amine). MS (EI): m/z = 446

(M^+). Theoretical values for elemental analysis: C, 64.56%; H, 4.06%; N, 31.37%; experimental values: C, 65.68%; H, 4.13%; N, 33.23%. ^{1}HNMR was measured at 500 MHz, DMSO-d, room temperature (Fig. S1).

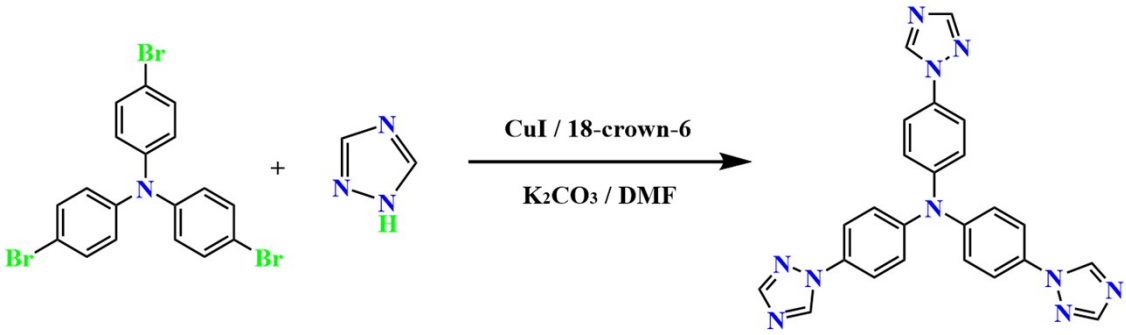

Fig. S1 Synthetic route of TTZ.

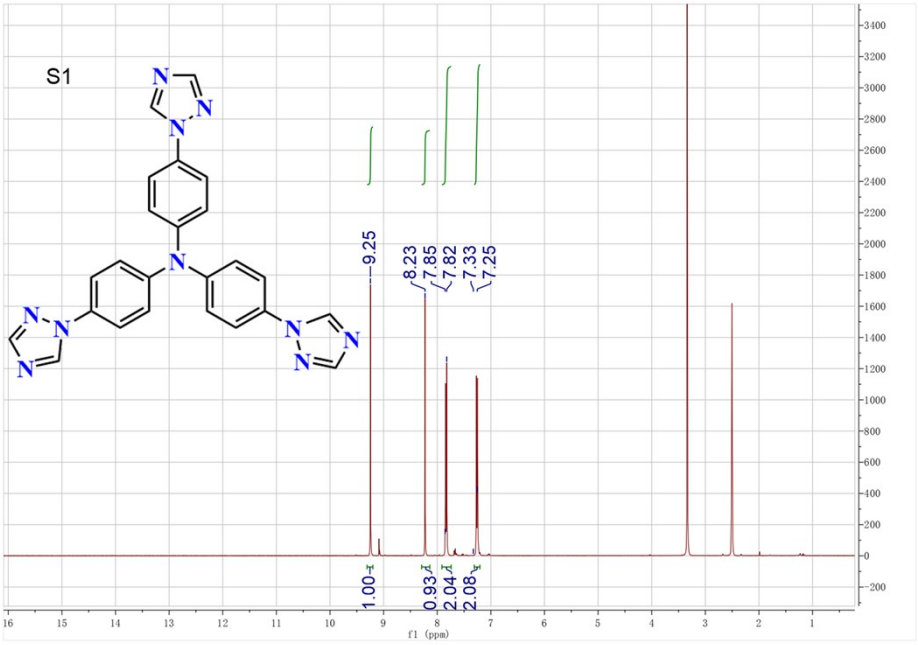

Fig. S2 NMR hydrogen spectra of TTZ.

Synthesis of TBA. A white thick solution was obtained by dissolving 9.68 g of 4-(bromomethyl)benzoic acid (45.0 mmol), 13.80 g of 4-(aminomethyl)benzoic acid (200.0 mmol), and 8.97 g of K_2CO_3 (65.0 mmol) in 250 mL of 1,4-dioxane solution. Vacuum was drawn and then N_2 was passed to ensure oxygen-free conditions, and the solution was heated at 160°C, condensed and refluxed for 3 days, and cooled to room temperature after 3 days. 1,4-dioxane was removed by rotary evaporator. Methanol

was added to the mixture after rotary evaporation, the crude product was dissolved and potassium carbonate was isolated by filtration. Spin evaporation of the methanol gave the crude product of TBA, which was then separated by column chromatography (petroleum ether/ethyl acetate = 10:1) to give a light yellow solid powder of 5.37 g (approx. 57% yield, based on 4-(bromomethyl)benzoic acid).MS (EI): m/z = 419 (M^+). Theoretical values of elemental analysis: C, 68.73%; H, 5.05%; N, 3.34%; O, 22.89%; experimental values: C, 69.11%; H, 4.93%; N, 3.15%. Fig. S4 shows the ^{1}HNMR (500 MHz, DMSO-d, room temperature) test spectrum of TBA.

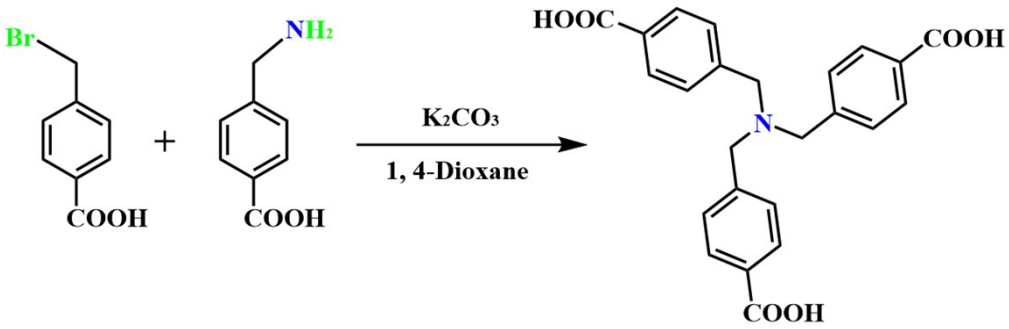

Fig. S3 Synthetic route of TBA.

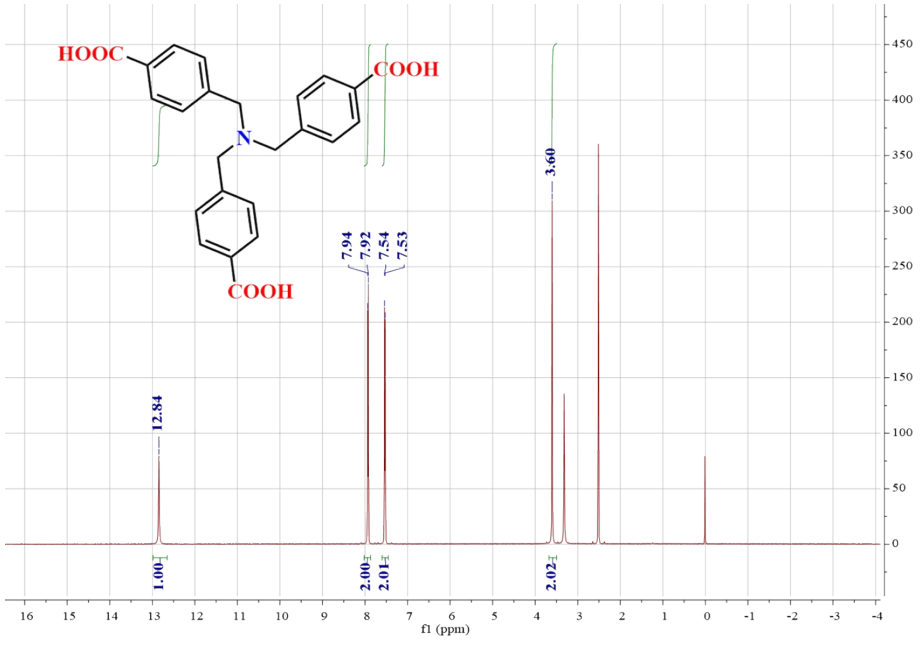

Fig. S4 NMR hydrogen spectra of TBA.

Synthesis of Co^1-MOF-1. A mixture of $Co(NO_3)_2$-$6H_2O$ (29.10 mg, 0.10 mmol), TTZ ligand 22.3 mg (0.05 mmol) was added to 4.5 mL of DMF: H_2O (v : v = 0.5 : 4) mixture, dissolved by ultrasonication and then put into a stainless steel reactor

equipped with a Teflon liner, and heated to react for three days at 95 °C, and then the reaction was After the reaction, it was cooled to room temperature. After washing and drying with the mother liquor, the light pink colored crystals could be observed under the microscopes which were clearly visible under a microscope. The yield was about 71%. Theoretical values for elemental analysis of Co^1-MOF-1 ($C_{52.5}H_{56.5}CoN_{24}O_{14}$): C, 48.22%; H, 4.32%; N, 25.71%; experimental values: C, 50.05%; H, 4.22%; N, 23.53%.

Synthesis of Co^8-MOF-2. A mixture of $Co(NO_3)_2$-$6H_2O$ (29.10 mg, 0.10 mmol), 20.95 mg (0.05 mmol) of TBA ligand was added to a mixture of DMF: ACN: H_2O (v: v: v = 2: 4: 2) and placed in a stainless steel high-pressure reactor at 95 °C for three days, and then cooled down to room temperature at the end of the reaction. The red lumpy crystals visible to the naked eye were washed with the mother liquor, and pure crystals were obtained after drying. The yield was about 63%. Theoretical values of elemental analysis of Co^2-MOF-2 ($C_{55}H_{59.5}Co_4N_{4.5}O_{19}$): C, 49.88%; H, 4.49%; N, 4.76%; experimental values: C, 51.46%; H, 4.14%; N, 4.35%.

Synthesis of Co^3-MOF-3. An appropriate amount of a mixture of crystals of Co^1-MOF-1 and crystals of Co^8-MOF-2 was added to 4 mL of a mixed solution of DMF:ACN:H_2O (v:v:v = 0.5:1.5:2). The two crystals were sonicated for 3 min for uniform distribution, and after sonication, they were heated in a reactor at 115 °C for three days. Subsequently, it was allowed to cool naturally to ambient temperature, and finally irregular massive crystals of reddish brown color were obtained from the conversion. The yield was about 59%. Theoretical values of elemental analysis of Co^3-MOF-3 ($C_{100.2}H_{92.2}Co_3N_{23.4}O_{18.6}$): C, 57.30%; H, 4.39%; N, 15.61%; experimental values: C, 58.75%; H, 4.64%; N, 15.88%.

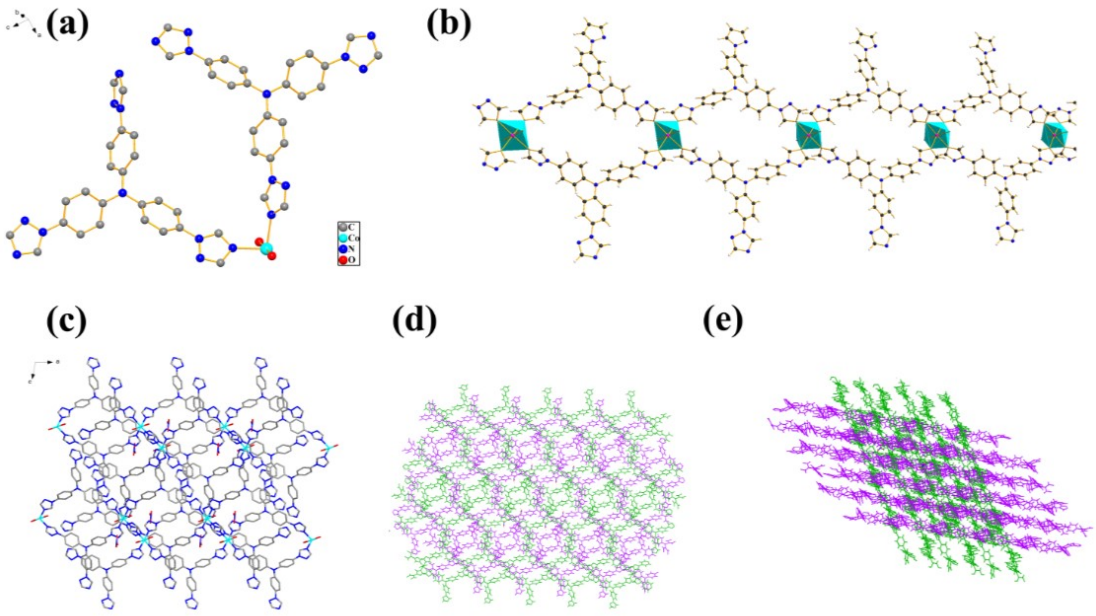

Fig. S5 (a) Asymmetric unit of Co^{1}-MOF-1; (b) one-dimensional chain structure of Co^{1}-MOF-1; (c) one-dimensional interpenetrating "Hopf chain " structure of Co^{1}-MOF-1; (d, e) Simplified topology of Co^{1}-MOF-1 in different directions.

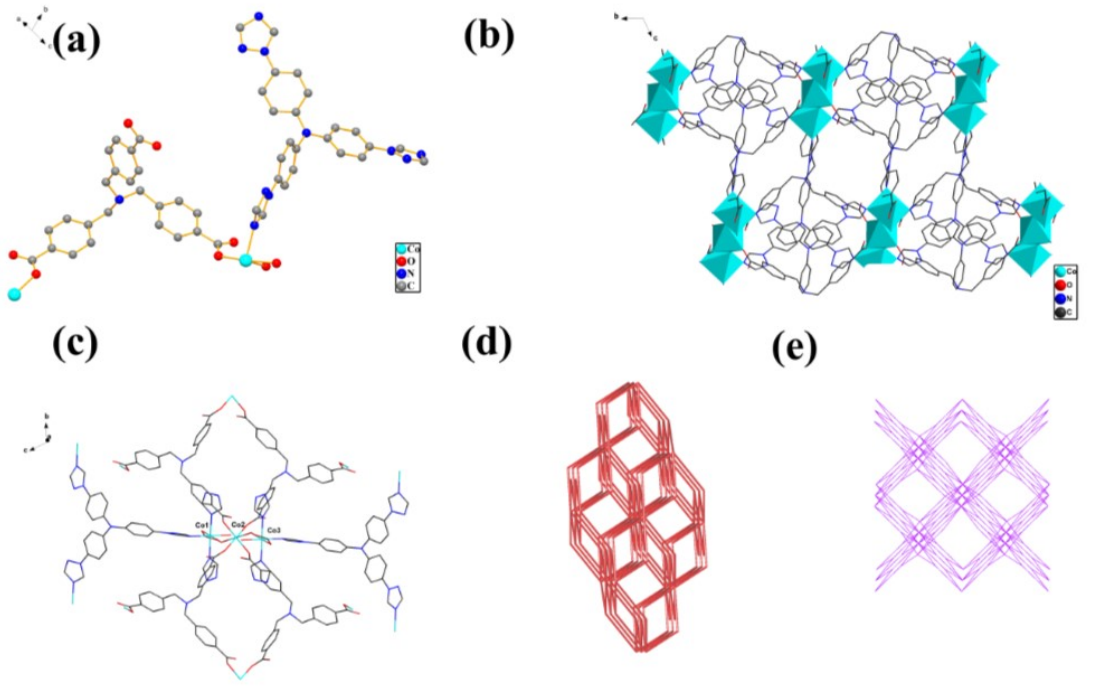

Fig. S6 (a) Asymmetric cell diagram of Co^{3}-MOF-3; (b) 3D network structure of Co^{3}-MOF-3; (c) linear triple-core Co cluster structure of Co^{3}-MOF-3; (d, e) simplified topology of Co^{3}-MOF-3 in different directions.

Table S1 Crystal data and structural refinement parameters of Co^{1}-MOF-1, Co^{8}-MOF-2 and Co^{3}-MOF-3

Complexes	Co^{1}-MOF-1	Co^{8}-MOF-2	Co^{3}-MOF-3
Chemical formula	$C_{52.5}H_{56.5}CoN_{24}O_{14}$	$C_{55}H_{59.5}Co_4N_{4.5}O_{19}$	$C_{100.2}H_{92.2}Co_3N_{23.4}O_{18.6}$
M_r	1306.64	1323.29	2098.56
Crystal system	Monoclinic	Triclinic	Triclinic
Space group	*C2/c*	*P***Error!**	*P***Error!**
Temperature (K)	293(2)	293(2)	293(2)
a / Å	29.491(6)	13.9685(17)	13.003(15)
b / Å	12.556(3)	15.694(2)	14.167(16)
c / Å	32.905(7)	17.408(2)	15.485(17)
α / °	90	63.516(2)	107.218(17)
β / °	100.794(4)	68.026(2)	114.473(18)
γ/ °	90	80.041(2)	98.439(18)
V / Å^3	11968(5)	3167.5(7)	2358(5)
Z	8	2	1
D_{calcd} / g cm^{-3}	1.450	1.387	1.478
Radiation type	Mo *K*α	Mo *K*α	Mo *K*α
λ / Å	0.71073	0.71073	0.71073
μ / mm^{-1}	0.373	1.100	0.607
Crystal size / mm	0.30 × 0.28 × 0.22	0.34 × 0.26 × 0.24	0.32 × 0.28 × 0.26
F(000)	5428	1362	1087
θ min−max / °	1.406−28.702	1.711−25.000	1.583−22.499
Tot., uniq. data	43187, 15202	17811, 11078	13107, 6016
R(int)	0.0444	0.0459	0.0874
*N*res, *N*par	51, 679	95, 724	27, 641
R_1, wR_2 [$I > 2\sigma(I)$]	0.0492, 0.1299	0.0532, 0.1258	0.0807, 0.2188
GOF on F^2	0.931	0.887	1.023
Largest diff. peak and hole (e·Å^{-3})	0.555 and -0.397	0.477 and -0.390	0.971 and -0.920

$R_1=\Sigma||F_o|-|F_c||/|\Sigma|F_o|$；$wR_2=\{\Sigma[w(F_o^2-F_c^2)^2]/\Sigma[w(F_o^2)^2]\}^{1/2}$；wherew=$1/[\sigma^2(F_o^2)+(aP)^2+bP]$,$P=(F_o^2+2F_c^2)/3$.

Table S2 Partial bond lengths (Å) of Complexes Co-MOFs

Co^{1}-MOF-1					
Co(1)-O(8W)	2.0706(16)	Co(1)-N(11)	2.1428(17)	Co(1)-N(1)#1	2.1858(16)

Co(1)-O(7W)	2.0708(15)	Co(1)-N(7)	2.1604(18)	Co(1)-N(17)#2	2.1956(16)
			Co^{8}-MOF-2		
Co(1)-O(2W)	2.105(3)	Co(2)-O(11)#3	2.266(3)	Co(3)-O(14)#6	2.107(3)
Co(1)-O(2)#1	2.322(3)	Co(2)-O(8)	2.071(3)	Co(3)-O(14)	2.065(3)
Co(1)-O(3)	2.062(4)	Co(2)-O(13)	2.008(3)	Co(4)-O(2)#4	2.106(3)
Co(1)-O(7)	2.034(3)	Co(2)-O(4)	2.035(4)	Co(4)-O(10)#7	2.166(3)
Co(1)-O(10)#2	2.123(3)	Co(3)-O(11)	2.122(3)	Co(4)-O(12)	2.070(3)
Co(1)-O(13)	2.013(3)	Co(3)-O(1)#4	2.098(3)	Co(4)-O(14)	2.030(3)
Co(2)-O(1W)	2.175(4)	Co(3)-O(9)#5	2.098(3)	Co(4)-O(3W)	2.122(3)
Co(2)-O(15)	2.069(4)	Co(3)-O(13)#3	2.088(3)	Co(4)-O(5)	2.107(3)
			Co^{3}-MOF-3		
Co(2)-O(5)	2.033(5)	Co(2)-N(2)	2.121(6)	Co(2)-O(7W)	2.128(5)
Co(2)-N(5)#1	2.121(6)	Co(2)-N(8)#2	2.174(6)	Co(2)-O(8W)	2.131(5)
Co(1)-O(2)	2.035(5)	Co(1)-O(2)#3	2.035(5)	Co(1)-O(3)#4	2.065(5)
Co(1)-O(3)#5	2.065(5)	Co(1)-(7W)#6	2.217(5)	Co(1)-O(7W)#7	2.217(5)

Table S3 Partial bond angle (°) of Complexes Co-MOFs

			Co^{1}-MOF-1		
O(11W)-Co(1)-(10W)	176.70(7)	O(11W)-Co(1)-N(7)	89.70(7)	N(11)-Co(1)-N(1)#1	89.45(7)
O(11W)-Co(1)-(17)#2	91.54(7)	O(10W)-Co(1)-N(11)	95.32(8)	N(11)-Co(1)-N(7)	177.42(7)
O(10W)-Co(1)-N(1)#1	90.14(7)	O(10W)-Co(1)-N(7)	87.08(8)	N(11)-Co(1)-N(17)#2	86.58(7)
O(11W)-Co(1)-N(1)#1	89.16(7)	O(10W)-Co(1)-(17)#2	89.38(7)	N(7)-Co(1)-N(1)#1	89.59(7)
O(11W)-Co(1)-N(11)	87.90(7)	N(1)#1-Co(1)-(17)#2	175.94(7)	N(7)-Co(1)-N(17)#2	94.41(7)
			Co^{8}-MOF-2		
O(2W)-Co(1)-O(2)#1	85.22(13)	O(13)-Co(1)-O(10)#2	92.57(11)	O(4)-Co(2)-O(8)	95.69(15)
O(2W)-Co(1)-O(10)#2	83.26(12)	O(1W)-Co(2)-O(11)#3	90.01(13)	O(1)#4-Co(3)-O(11)	95.06(13)
O(3)-Co(1)-O(2W)	92.77(14)	O(15)-Co(2)-O(1W)	86.77(17)	O(1)#4-Co(3)-O(14)#6	88.91(12)
O(3)-Co(1)-O(2)#1	172.99(13)	O(15)-Co(2)-O(11)#3	93.05(13)	O(9)#5-Co(3)-O(11)	97.29(13)
O(3)-Co(1)-O(10)#2	91.82(13)	O(15)-Co(2)-O(8)	92.15(15)	O(9)#5-Co(3)-O(1)#4	87.03(13)
O(7)-Co(1)-O(2W)	89.82(13)	O(8)-Co(2)-O(1W)	85.36(15)	O(9)#5-Co(3)-O(14)#6	87.85(12)
O(7)-Co(1)-O(2)#1	93.35(13)	O(8)-Co(2)-O(11)#3	172.84(14)	O(13)#3-Co(3)-O(11)	79.70(12)
O(7)-Co(1)-O(3)	93.36(15)	O(13)-Co(2)-O(1W)	85.78(14)	O(13)#3-Co(3)-O(1)#4	174.57(13)
O(7)-Co(1)-O(10)#2	171.55(13)	O(13)-Co(2)-O(15)	168.35(14)	O(13)#3-Co(3)-O(9)#5	92.20(12)
O(10)#2-Co(1)-O(2)#1	81.28(11)	O(13)-Co(2)-O(11)#3	78.02(11)	O(13)#3-Co(3)-O(14)#6	96.44(11)
O(13)-Co(1)-O(2W)	165.44(13)	O(13)-Co(2)-O(8)	96.16(13)	O(14)-Co(3)-O(11)	92.30(12)
O(13)-Co(1)-O(2)#1	80.35(12)	O(13)-Co(2)-O(4)	96.64(14)	O(14)#6-Co(3)-O(11)	173.65(12)
O(13)-Co(1)-O(3)	101.32(13)	O(4)-Co(2)-O(1W)	177.23(15)	O(14)-Co(3)-O(1)#4	92.75(12)
O(13)-Co(1)-O(7)	92.96(13)	O(4)-Co(2)-O(15)	90.63(16)	O(14)-Co(3)-O(9)#5	170.39(12)
O(14)-Co(3)-O(13)#3	88.91(11)	O(4)-Co(2)-O(11)#3	89.18(13)	O(14)-Co(4)-O(3W)	173.40(12)
O(14)-Co(3)-O(14)#6	82.54(11)	O(12)-Co(4)-O(10)#7	172.32(12)	O(14)-Co(4)-O(5)	88.45(11)

O(2)#4-Co(4)-O(10)#7	85.42(12)	O(12)-Co(4)-O(3W)	86.38(13)	O(3W)-Co(4)-O(10)#7	86.84(12)
O(2)#4-Co(4)-O(3W)	82.98(12)	O(12)-Co(4)-O(5)	89.72(13)	O(5)-Co(4)-O(10)#7	94.20(12)
O(2)#4-Co(4)-O(5)	175.62(12)	O(14)-Co(4)-O(2)#4	95.88(12)	O(5)-Co(4)-O(3W)	92.64(13)
O(12)-Co(4)-O(2)#4	90.16(13)	O(14)-Co(4)-O(10)#7	86.58(11)	O(14)-Co(4)-O(12)	100.14(12)
		Co^3-MOF-3			
O(5)-Co(2)-N(5)#1	91.5(2)	O(5)-Co(2)-N(2)	88.8(2)	N(5)#1-Co(2)-N(2)	88.4(2)
O(5)-Co(2)-O(7W)	174.50(18)	N(5)#1-Co(2)-O(7W)	92.0(2)	N(2)-Co(2)-O(7W)	95.5(2)
O(5)-Co(2)-O(8W)	92.1(2)	N(5)#1-Co(2)-O(8W)	91.3(2)	N(2)-Co(2)-O(8W)	179.1(2)
O(7W)-Co(2)-O(8W)	83.6(2)	O(5)-Co(2)-N(8)#2	92.4(2)	N(5)#1-Co(2)-N(8)#2	176.0(2)
N(2)-Co(2)-N(8)#2	91.0(2)	O(7W)-Co(2)-N(8)#2	84.1(2)	O(8W)-Co(2)-N(8)#2	89.2(2)
O(2)-Co(1)-O(2)#3	180.0(3)	O(2)-Co(1)-O(3)#4	93.1(2)	O(2)#3-Co(1)-O(3)#4	86.9(2)
O(2)-Co(1)-O(3)#5	86.9(2)	O(2)#3-Co(1)-O(3)#5	93.1(2)	O(3)#4-Co(1)-O(3)#5	180.0
O(2)-Co(1)-O(7W)#6	93.0(2)	O(2)#3-Co(1)-O(7W)#6	87.0(2)	O(3)#4-Co(1)-O(7W)#6	89.1(2)
O(3)#5-Co(1)-(7W)#6	90.9(2)	O(2)-Co(1)-O(7W)#7	87.0(2)	O(2)#3-Co(1)-O(7W)#7	93.0(2)
O(3)#4-Co(1)-(7W)#7	90.9(2)	O(3)#5-Co(1)-O(7W)#7	89.1(2)	O(7W)#6-Co(1)-(7W)#7	180.0

Symmetry Codes for Co^1-MOF-1: #1 x-1/2,y-1/2,z; #2 x+1/2,y+1/2,z; #3 -x+1,y,-z+1/2.

Symmetry Codes for Co^8-MOF-2: #1 x,y+1,z; #2 x,y,z-1; #3 -x+1,-y+1,-z+1; #4 x,y,z+1; #5 -x+1,-y+1,-z+2; #6 -x+1,-y,-z+2; #7 x,y-1,z.

Symmetry Codes for Co^3-MOF-3: #1 x,y,z-1; #2 x-1,y-1,z-1; #3 -x+1,-y+2,-z+2; #4 -x+1,-y+1,-z+2; #5 x,y+1,z; #6 x,y+1,z+1; #7 -x+1,-y+1,-z+1

Preparation of working electrodes: A mixture of 990 μL of ethanol and 10 μL of Nafion D-521 dispersion was used to disperse 2 mg of photocatalyst to prepare a homogeneous slurry. Two hundred microlitres of the paste was uniformly coated on a 1 cm × 2 cm sized indium tin oxide (ITO) glass sheet and allowed to dry naturally at room temperature. In the experiments, a silver/silver chloride electrode was used as the reference electrode, while a platinum plate served as the counter electrode.

Electrochemical testings: All electrochemical measurements (including photocurrent and Mott Schottky tests) were performed using a conventional three-electrode system and in 0.2 M Na_2SO_4 aqueous solution at pH=7. The CHI 660E electrochemical workstation was used with the working electrode of the CHI 660E electrochemical workstation as an ITO glass plate with electrode photocatalyst slurry, a platinum foil for the counter electrode, and electrolyte silver/silver chloride electrodes. In addition, it was carried out at AC frequencies of 500 Hz, 1000 Hz and 1500 Hz. Mott-Schottky

diagram measurements. All three electrodes were located in 0.2 M Na_2SO_4 aqueous solution.

Photocatalytic reduction of carbon dioxide experiment: Firstly, 100 mg of catalyst was placed in an argon atmosphere at a specific temperature and calcined in a vacuum tube furnace for 2 h to obtain an activated catalyst sample. Next, 5 mg of the activated catalyst and the photosensitiser ruthenium tripyridyl were added into a photocatalytic reactor, and 5 ml of triethylamine and 20 ml of acetonitrile solvent were sequentially injected as the reaction medium. Then, the system was continuously bubbled through high-purity CO_2 gas for about 20 min to effectively remove oxygen and other residual gases from the system.

After the preparation, the photoreactor was illuminated using a xenon lamp (MC-PF300C) equipped with a 400 nm filter to start the photocatalytic reaction, while a condensate was injected to maintain a stable temperature of the reaction system. At the end of the experiment, the generated gaseous products were collected and quantitatively analysed by gas chromatography, while the liquid products were further characterised by mass spectrometry to determine the generated species and reaction efficiency.

2. Experimental data.

Crystal structure determination: SCXRD tests were conducted on a Bruker SMART APEX CCD diffractometer using Mo K_α radiation. The structure was solved by the *SHELXT*[1] structure solution program using intrinsic phasing method and refined by full matrix least squares on F^2 using *SHELXL*[2,3] implanted in *Olex*2.[4] All non-hydrogen atoms were refined anisotropically. Hydrogen atom positions were calculated geometrically and refined using the riding model. The removal of the contributions from disordered solvent molecules and anions were calculated by *PLATON*/*SQUEEZE* routine.[5] Crystallographic data in CIF format of Co^1-MOF-1, Co^8-MOF-2 and Co^3-MOF-3 have been deposited in the Cambridge Crystallographic Data Centre (CCDC) under deposition CCDC numbers: 2372225-2372227. The details of crystal parameters, data collection, and refinements for Co^1-MOF-1, Co^8-MOF-2 and Co^3-MOF-3 are summarized in Table S1. Selected bond lengths and angles are given in Table S2 and S3.

Additional data collection and refinement details:

Co[1]-MOF-1: For the NO_3^- anion in the structure, **SIMU 0.01 0.02** as well as **ISOR 0.01 0.02** commands were used on all 4 atoms to obtain better thermal ellipsoids. The geometry of NO_3^- anion was fixed by applying three DFIX commands (**DFIX 1.24 0.01 O3 N21 O2 N21 O1 N21; DFIX 1.25 0.01 O3 N21 O1 N21 O2 N21; DFIX 2.16 0.01 O1 O3 O2 O3 O1 O2**). A solvent mask was calculated and 1066 electrons were found in a volume of 3508 Å^3 in 1 void per unit cell. This is consistent with the presence of 1.5 NO_3^-, 1.5 DMF, 3 H_2O per Asymmetric Unit which account for 1092 electrons per unit cell.

Co[8]-MOF-2: For the disordered DMF in the asymmetric unit, two orientations of the ligands can be assigned and splitted into two parts. The refined occupancies were 0.75 and 0.25. **SIMU 0.01 0.02** was used to obtain better thermal ellipsoids. The geometry of disordered DMF molecule was fixed by applying additional commands (**SADI C49A C50A C49B C50B; SADI C50A C51A C50B C51B; SADI O15 C49B O15 C49A; DFIX 1.36 0.01 N3A C49A N3B C49B; DFIX 1.45 0.01 N3B C50B N3A C50A N3B C51B N3A C51A**). A solvent mask was calculated and 103 electrons were found in a volume of 815 Å^3 in 1 void per unit cell. This is consistent with the presence of 0.5 CH_3CN, 1 DMF per Asymmetric Unit which account for 102 electrons per unit cell.

Co[3]-MOF-3: The resolution was cut to 2*theta* = 45° based on the plot of $CC_{1/2}$ *vs*. resolution plot and some disagreeable reflections were omitted. Looking at the residual map, there is a negative hole over Co1, which is sat on a symmetry element. When freely refined the occupancy is around ~85%. However a lower occupancy seems unlikely given the nature of the structure and another element is also not reasonable given the nature of formation so it has been left fully occupied. For the disordered triazole ring in the asymmetric unit, two orientations of the ligands can be assigned and splitted into two parts. The refined occupancies were 0.63 and 0.37.

ISOR 0.01 0.02 command was used on the disordered part to obtain better thermal ellipsoids. The geometry of disordered triazole was fixed by applying additional commands (**SADI 0.01 N9 N10B N9 N10A, SADI 0.01 N10B C42B N10A C42A, SADI 0.01 N8 C42B N8 C42A**). A solvent mask was calculated and 68 electrons were found in a volume of 349 $Å^3$ in 2 voids per unit cell. This is consistent with the presence of 1.4 DMF, 1.2 H_2O per Asymmetric Unit which account for 68 electrons per unit cell.

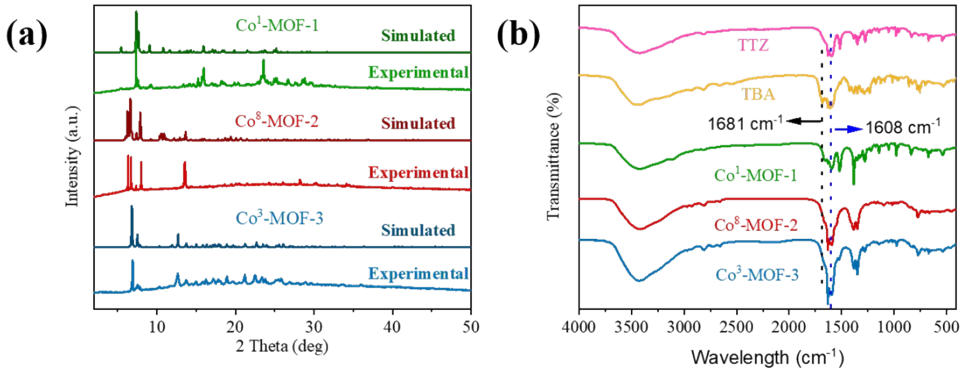

Fig. S7 PXRD and IR maps of Co-MOFs. (a) Simulated and experimentally obtained XRD plots of Co-MOFs; (b) IR spectra of ligands TTZ and TBA and Co-MOFs

PXRD Analysis: The experimental PXRD patterns of Co^1-MOF-1, Co^8-MOF-2, and Co^3-MOF-3 are in excellent agreement with their respective simulated patterns from single-crystal data (Fig. S7a). This confirms that the bulk synthesized materials are pure and crystalline, and that the SCSC transformation to Co^3-MOF-3 proceeds without compromising the crystallinity of the product phase. The distinct diffraction patterns for each MOF provide clear evidence of their different crystal structures and successful phase transitions.

FTIR Analysis: FTIR spectroscopy (Fig. S7b) confirms the successful incorporation of the TTZ and TBA ligands into the MOF frameworks. The disappearance of the characteristic C=O stretching vibration (~1681 cm^{-1}) of TBA in all MOFs indicates carboxylate deprotonation and subsequent coordination to Co^{2+} ions. Concurrently, a redshift of the C–N stretching vibration (1608 cm^{-1}) from the TTZ ligand verifies the coordination of its nitrogen atoms to the metal centers. Critically, the distinct FTIR profile of Co^3-MOF-3, which differs from both Co^1-MOF-1 and Co^8-MOF-2,

provides vibrational evidence for the formation of a unique coordination environment following the SCSC transformation.

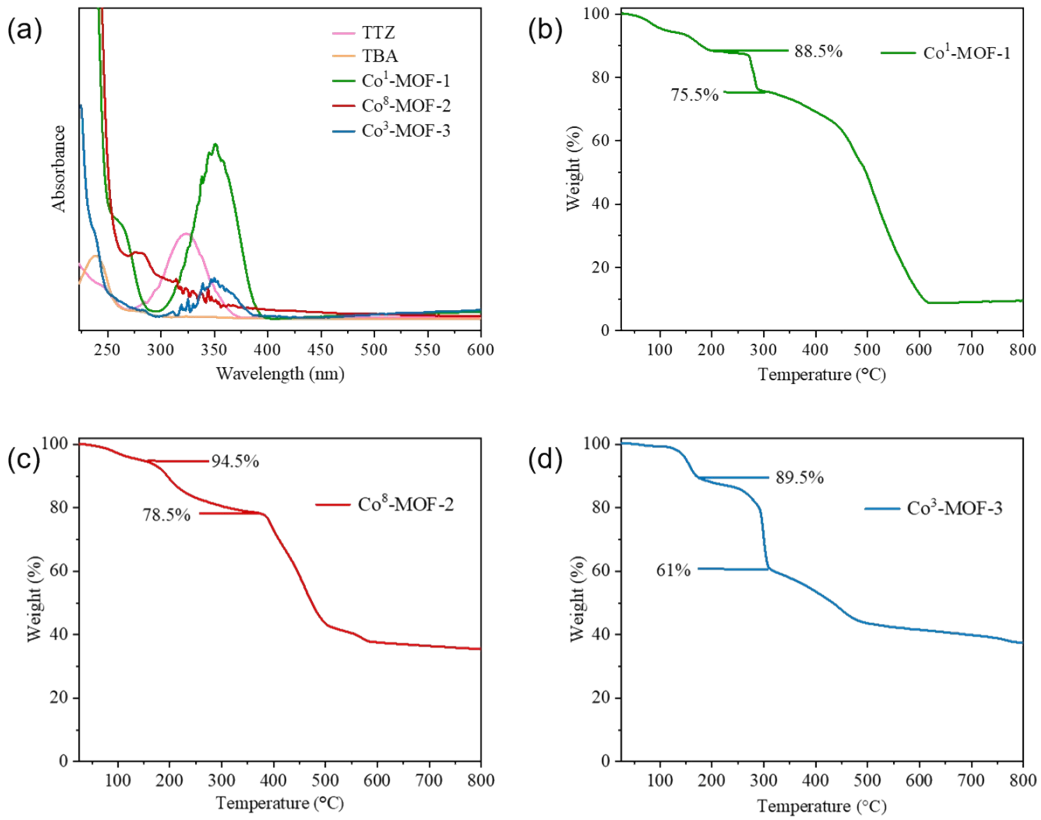

Fig. S8 UV-Vis of ligands TTZ and TBA and Co-MOFs and TGA plots of Co-MOFs. (a) UV-visible absorption spectra of ligands TTZ and TBA and Co-MOFs; (b) thermogravimetric analysis profile of Co^1-MOF-1; (c) thermogravimetric analysis profile of Co^8-MOF-2; and (d) thermogravimetric analysis profile of Co^3-MOF-3

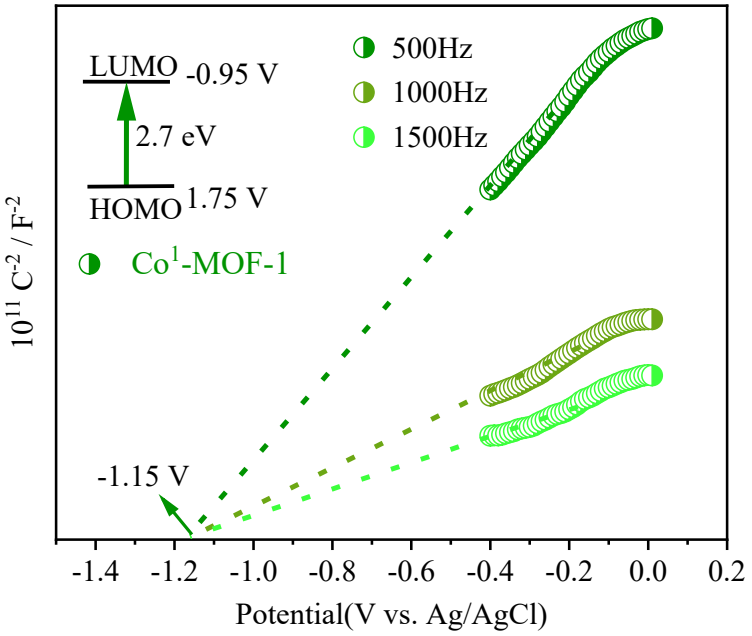

Fig. S9 Mott-Schottky plot for Co^1-MOF-1

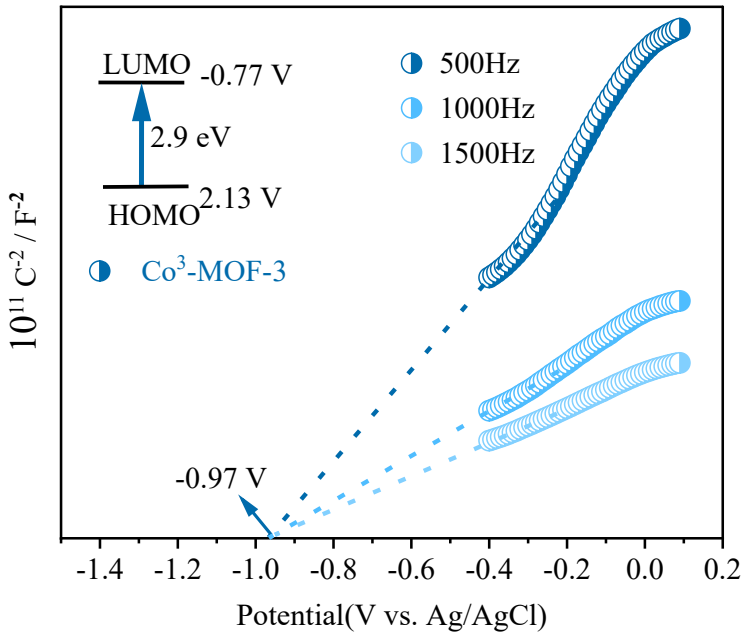

Fig. S10 Mott-Schottky plot for Co^3-MOF-3

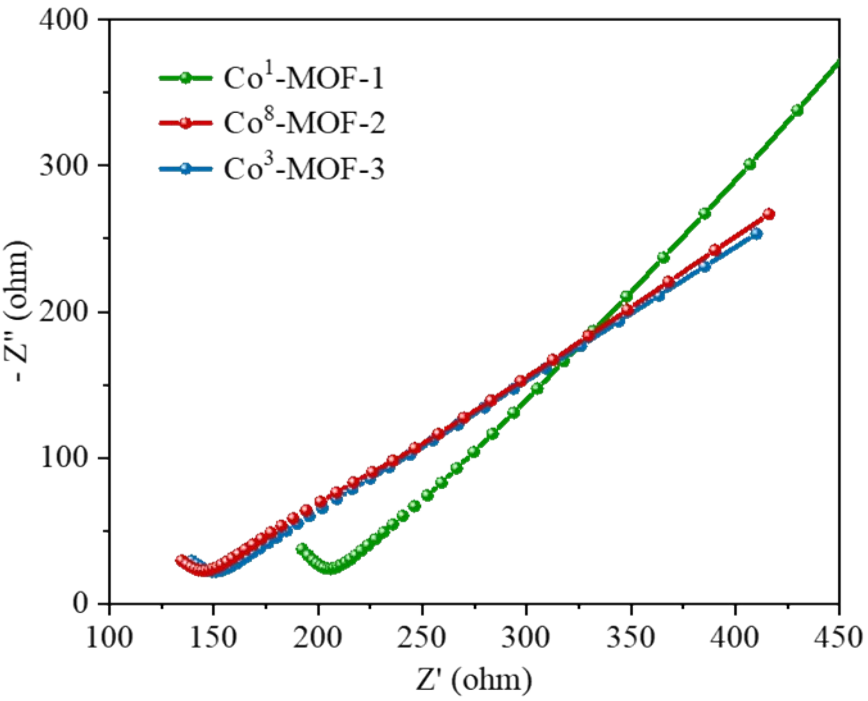

Fig. S11 ESI impedance maps of Co-MOFs.

References

1. Sheldrick, G. M. SHELXT – Integrated Space-Group and Crystal-Structure Determination. *Acta Crystallogr. Sect. A Found. Adv*. **2015**, *71*, 3–8.
2. Sheldrick, G. M. A Short History of SHELX. *Acta Crystallogr. Sect. A Found. Crystallogr*. **2008**, *64*, 112–122.
3. Sheldrick, G. M. Crystal Structure Refinement with SHELXL. *Acta Crystallogr. Sect. C Struct. Chem*. **2015**, *71*, 3–8.
4. Dolomanov, O. V; Bourhis, L. J.; Gildea, R. J.; Howard, J. A. K.; Puschmann, H. OLEX2: A Complete Structure Solution, Refinement and Analysis Program. *J. Appl. Crystallogr*. **2009**, *42*, 339–341.
5. Spek, A. L. PLATON SQUEEZE: A Tool for the Calculation of the Disordered Solvent Contribution to the Calculated Structure Factors. *Acta Crystallogr. Sect. C, Struct. Chem*. **2015**, *71*, 9–18.